

GT2011-45&++

NUMERICAL COMPARISON OF HEAT TRANSFER AND PRESSURE DROP IN GAS TURBINE BLADE COOLING CHANNELS WITH DIMPLES AND RIB-TURBULATORS

R.S. Amano

University of Wisconsin-Milwaukee
Milwaukee, WI, USA

Sourabh Kumar

University of Wisconsin-Milwaukee
Milwaukee, WI, USA

Krishna S. Guntur

University of Wisconsin-Milwaukee
Milwaukee, WI, USA

Jose Martinez Lucci

University of Wisconsin-Milwaukee
Milwaukee, WI, USA

ABSTRACT

In order to enhance the performance of a gas turbine and to maintain the blade material within operating temperature range, cooling channels are made within the blade materials that extract the heat. The walls of these cooling channels are usually enhanced with some sort of turbulence generators – ribs and dimples being the most common. While both the geometries provide improvement in enhancing the heat transfer, dimples usually have a lower pressure drop. It is essential to improve the heat transfer rate with a minimal pressure loss. In this study, the heat transfer and pressure loss are determined numerically and combined to show the effect of both in channels with ribs and dimples on one wall of the channel. Similar geometric and boundary conditions are used for both the turbulators. Reynolds numbers of 12,500 and 28,500, based on the hydraulic diameter are used for the study. The Reynolds-Stress Model was used for all the computations as a turbulence model by employing Fluent.

NOMENCLATURE

c_p	-	Specific heat at const. pressure
D_h	-	Hydraulic Diameter
e	-	Height of the ribs
f	-	Friction factor
f_0	-	Friction factor calculated from empirical relations
h	-	Convection heat transfer coefficient
k_{therm}	-	Thermal Conductivity
k_p	-	Turbulent Kinetic Energy at node point next to the wall ‘p’
Nu	-	Nusselt Number
Nu_o	-	Nusselt Number of smooth wall
P	-	P-Function [3]
‘p’	-	This is the node point next to the wall
\dot{q}_w	-	Rate of heat flux at the wall
Re_D	-	$= (U \cdot D_h / \nu)$ Reynolds number
T	-	Temperature
U	-	Free stream velocity
U_p	-	Mean velocity at node ‘P’
ν	-	Kinematic viscosity

Greek Symbols

ρ	-	Density
σ	-	Prandtl Number
σ_T	-	Turbulent Prandtl number
τ_w	-	Wall shear stress

Subscripts

D	-	Based on Hydraulic Diameter
w	-	Parameters at the wall

INTRODUCTION

Increasing inlet temperatures in gas turbine engines is possible due to the internal cooling technology. Cooling channels made within the blade material circulate coolant (air, water, steam etc.) to extract the heat and keep the blade material within operating range. Different geometries have been developed in order to enhance turbulence within the channel and thereby increase the heat transfer. Turbulence enhancers such as ribs and dimples have been placed on one wall of the channel to achieve higher heat transfer rate.

Bunker [1] reported the effect of different turbulence generators such as ribs, dimples and trenches and also discussed film cooling. He also investigated the effect of inline and staggered Chevron strips to improve the heat transfer compared to smooth walls. Full length pins and short pins were also discussed in the report. It was concluded that the full length pins provided higher heat transfer which might be attributed to the increased surface area.

Iacovides et al. [2] studied experimentally heat transfer rate in U-Bend channels with smooth walls and some turbulence generators. They studied both stationary and rotating channels for different geometries such as square, rectangular and a combination of both. They also reported about numerical computation of heat transfer in cooling channels using various turbulence models. Computational results of rib roughened channels of varying angles were reported in the paper [2].

Ekkad et al. [3] reported experimental measurement of wall Nusselt number distributions for various rib configurations in a U-bend square channel, with bleed holes. 60° standard ribs, 60° V-shaped ribs

and 60° inverted V-shaped ribs were studied by them. Based on the results they recommended using V-shaped ribs in the first pass and inverted V-shaped ribs in the second pass for the highest heat transfer rate.

Kim et al. [4] studied mass transfer characteristics in channel with 90° and 45° ribs in a square single pass channel with bleed holes. Naphthalene sublimation was used to measure mass transfer characteristics and thereby calculated the heat transfer by using the heat/mass transfer analogy. The case with 45° ribs did not show much change in heat/mass transfer compared to 90° ribs in a stationary channel. However, rotation induced secondary flows cause changes in turbulence and hence in heat/mass transfer.

Dimples are another widely used turbulence generators. Concave dimples on the channel walls provide turbulence while minimizing the frictional loss. Han and Ekkad [5] studied the effect of dimples in a high aspect ratio channel, with bleed holes. Nusselt number distributions for different Reynolds numbers were reported.

Zhou and Acharya [6] compared mass transfer by naphthalene sublimation of dimpled channel at different Reynolds numbers. It is concluded in their study that heat transfer was enhanced by a factor of 2 compared to a smooth channel.

Moon et al. [7] reported heat transfer and flow characteristics in a square channel with dimples, with varying channel height.

Although it is an established fact that dimples provide a lower frictional loss, there is not much literature quantitatively comparing dimples with ribs in similar flow conditions. In this study, computational result from a rib configuration is compared with the experimental results obtained from Ekkad et al. [3] to validate turbulence models. From previous publications by the authors [9-11], the RSM model was reported to predict results closer to the experimental data compared to k- ϵ and k- ω turbulence models and hence the RSM is chosen for this study. Using the RSM as the turbulence model, same heat transfer surface area and the same inlet and boundary conditions, Nusselt

number and friction factor distributions between the ribbed channels and the dimpled channels are compared. This shows a quantitative difference between dimples and ribs.

GEOMETRIC MODELS

Figure 1 shows the different geometries used in this study and Table 1 gives the geometric dimensions. Table 2 has the flow conditions used for the numerical analysis. The dimensions and the boundary conditions are set to be the same for the experimental study of Ekkad et al. [3]. An inlet channel was used to calculate the fully developed flow velocity, as done for the experiment [3]. The velocity at the inlet to this channel was calculated based on the Reynolds number and the hydraulic diameter of the channel.

Dimensions for the dimpled channel are obtained such that the ratio of the total areas of modified wall to the plane wall is the same as that of the ribbed channel. This includes the three surfaces of each rib and the surface area of the rectangular wall. The number of dimples is calculated to correspond to the same total area for the ribbed channel. Details are given in Eq (1) and (2).

For one pitch length (rib to rib),

$$\begin{aligned} \text{Area of ribbed wall} &= 32.04 + 3(0.63 \times 5.08) \\ &= 41.64 \text{ cm}^2 \end{aligned}$$

$$\begin{aligned} \text{Area of dimpled wall} &= \text{Area of ribbed wall} - (1) \\ N \left(\frac{1}{2} 4\pi r^2 \right) &= 41.64 \text{ cm}^2 \quad - (2) \end{aligned}$$

Taking the radius of the dimple to be the same as that of the bleed hole, i.e., $r = 0.63 \text{ cm}$, and we get, $N = 16.34 \sim 16$ per one pitch (6.3cm)

Table 1: Dimensions of the geometry

Cross section of the channel	5.08cm × 5.08 cm
Hydraulic Diameter (D_h)	5.08 cm
Length of the channel	11 D_h
Length of the inlet channel (not shown here, used to calculate fully developed	10 D_h

velocity profile)	
Height of the ribs (e)	0.22cm
Pitch of the ribs	10e
Angle of the ribs	60°
Diameter of the bleed holes	1.26 cm
Diameter of the dimples	1.26 cm
Number of dimples	16 per pitch length

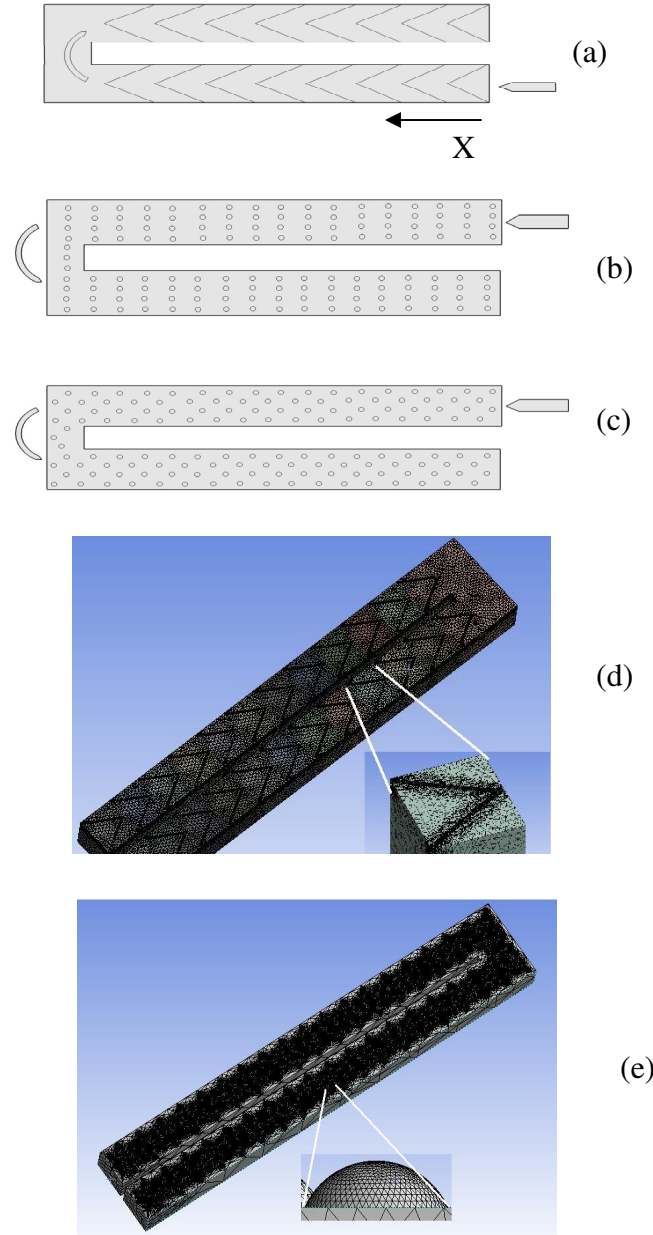


Figure 1: Schematic of different channel geometries and meshes used in this study

- (a) V-shape ribs, (b) dimples inline, (c) dimples in staggered array, (d) meshes for ribbed channel, (e) meshes for dimpled shape.

16 dimples (per pitch length) are distributed uniformly over the surface. Two different dimpled channels are used, one with a straight dimple-array and the other with a staggered dimple arrangement as shown in Figs. 1(b) and 1(c). The staggered arrangement has the adjacent line of dimples one diameter offset from the previous line.

Table 2: Flow conditions used

Reynolds Number	12,500	28,500
Inlet Velocity	3.59m/s	8.20m/s
Inlet Temperature	200°C	200°C
Constant wall temperature	27°C	27°C

The mesh used for the simulations was achieved after grid independence tests. For the dimples, mesh 1, mesh 2 and mesh 3 with 1.2, 1.7 and 1.9 million grid points, respectively, were used and tested for a grid independence based on both the mean velocity and the mean Nusselt number. Less than 2% change was observed in the results from mesh 2 and mesh 3. Therefore, mesh 2 was selected, having 1.7 million grid points. Similarly, 1.0, 1.2 and 1.5 million grid points were tested in the ribbed channel. Having less than 2% change compared to the grid with 1.5 million, the second mesh with 1.2 million grid points was selected. The average y^+ for this mesh is 25 due to the adoption of the standard wall function rather than the use of a low-Reynolds number model.

RESULTS AND DISCUSSION

The Nusselt number distribution shown here is calculated based on the shear stress as opposed to calculating from the energy equation (available in Fluent). From previous study [12], the shear stress calculation predicted results closer to the

experimental values compared to the energy equation. This comparison is shown in Fig. 3.

The shear-stress method was proposed by Amano [13] and is briefly reproduced here.

The near-wall variation in temperature and the local heat flux adopted are related as

$$\frac{\rho c_p (T - T_w) k_p^{1/2}}{\dot{q}_w''} = \left(\frac{U_p k_p^{1/2}}{\tau_w / \rho} + P \right) \quad \text{-----(3)}$$

where P is the P-Function given by Jayatilleke [3]. The p-function is defined as

$$P = 9.24 \left[(\sigma / \sigma_T)^{0.75} - 1 \right] \left[1 + 0.28 \exp(-0.007 \sigma / \sigma_T) \right] \quad (4)$$

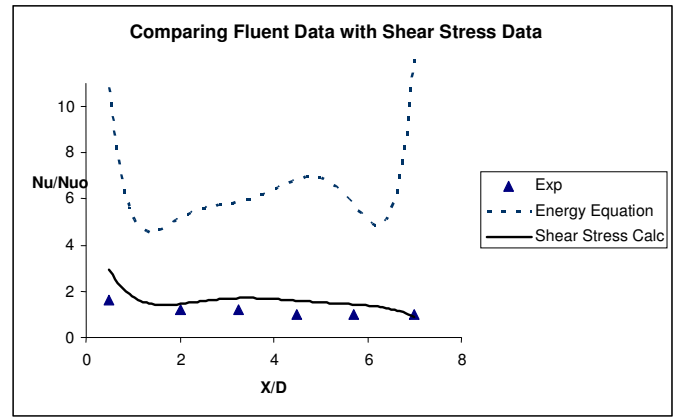


Figure 3: Comparison of shear stress calculation against energy equation [12]

In Eq. (3), the term, $(T - T_w) / \dot{q}_w''$ is to be recognized as the inverse of 'h', the convective heat transfer coefficient.

And the Nusselt number can be calculated as

$$Nu = \frac{h D_h}{k_{therm}} \quad \text{-----(5)}$$

where, D_h is the hydraulic diameter and k_{therm} is the thermal conductivity of the fluid (air in this case).

Shear stress values at the wall and velocity values at a distance of 6ϵ - $4D$ from the wall were obtained from the simulations. Then, the Nusselt number was calculated using Eqs. (3), (4) and (5) at each point. In the vicinity of the dimples, very low velocities are recorded due to flow circulations. This causes a very high Nusselt number in those areas. As only the Nusselt number distributions are

available from the experiment, only trends were observed rather than the actual distribution. For comparison, Nusselt number was normalized with the Dittus-Boelter relation [9].

$$Nu_o = 0.023 Re_D^{4/5} \sigma^{0.4} \quad \text{-----(6)}$$

Figure 4 shows the Nusselt number distribution for the three channels at $Re_D=12,500$. Figure 5 shows the same at $Re_D=28,500$. It is evident from these figures, that Nusselt number distributions for all three configurations are similar. The heat transfer is noticeably increasing after the turn, $X/D = 0$. The channel with ribs shows slightly increased overall heat transfer compared to the channels with dimples.

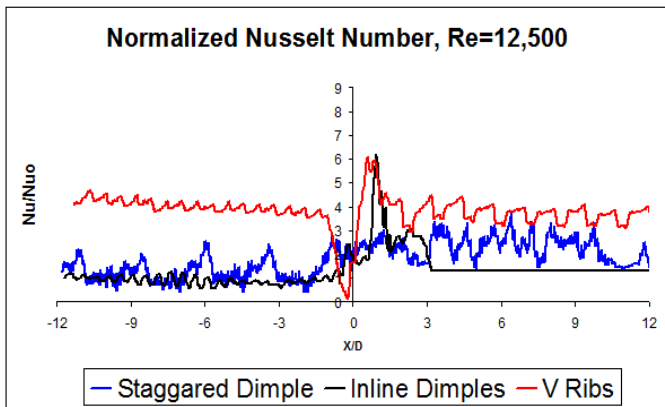


Figure 4: Normalized Nusselt Number distribution along the length of the channel for the three geometric configurations, at $Re=12,500$

Figures 6 and 7 show the normalized skin friction coefficient for the various channels at $Re = 12,500$ and $Re = 28,500$, respectively. It is quite evident that the ribbed channel has much higher skin friction as expected. On an average, the friction in ribbed channel is about five times higher than that from the dimpled channel. All the channels show lower skin friction downstream of the bend compared upstream. This might be due to increased turbulence. The Coriolis forces acting in the bend section push the flow outward. The distributions show periodic peaks which are due to the periodic nature of the geometry for both ribs and dimples.

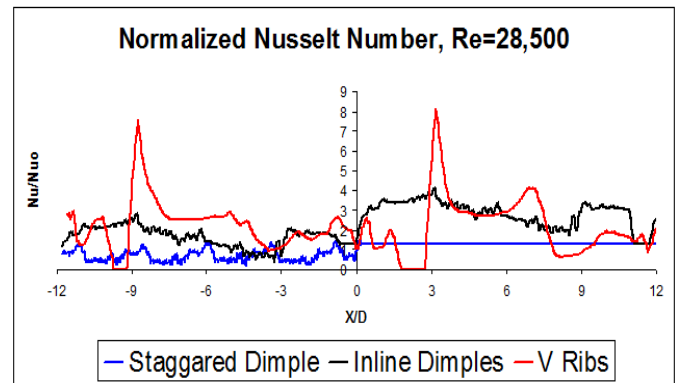


Figure 5: Normalized Nusselt Number distribution along the length of the channel for the three geometric configurations, at $Re=28,500$

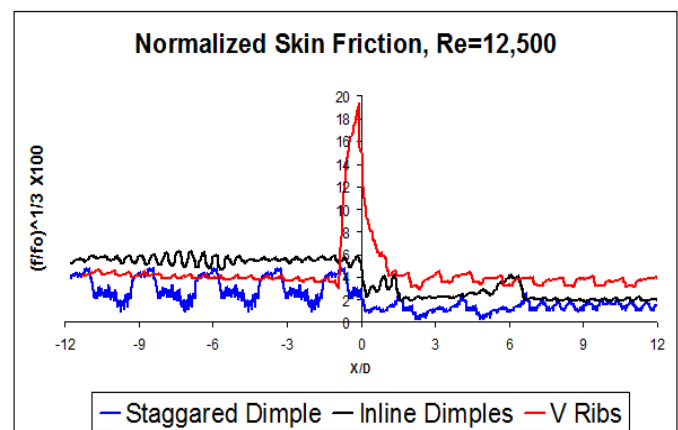


Figure 6: Normalized Skin Friction distribution along the length of the channel for the three geometric configurations, at $Re=12,500$

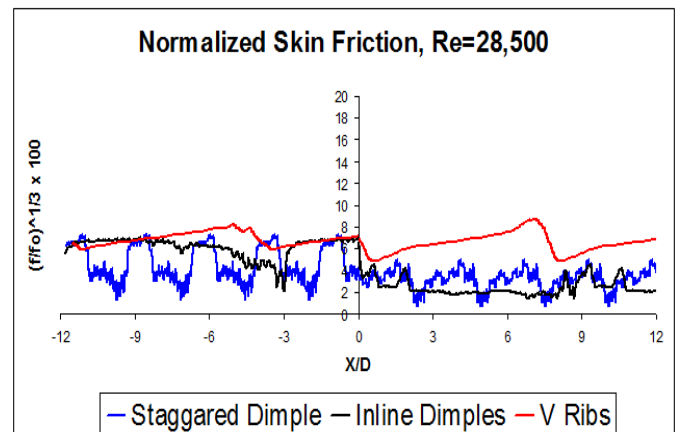


Figure 7: Normalized Skin Friction distribution along the length of the channel for the three geometric configurations, at $Re=28,500$

To better understand the effect of both heat transfer and friction loss, the ratio of normalized Nusselt number to normalized skin friction factor is

calculated for all the three channels and is referred to as the “channel effectiveness”.

$$\text{Channel Effectiveness, } \varepsilon_{\text{channel}} = \frac{Nu/Nu_o}{(f/f_o)^{1/3}} \quad (6)$$

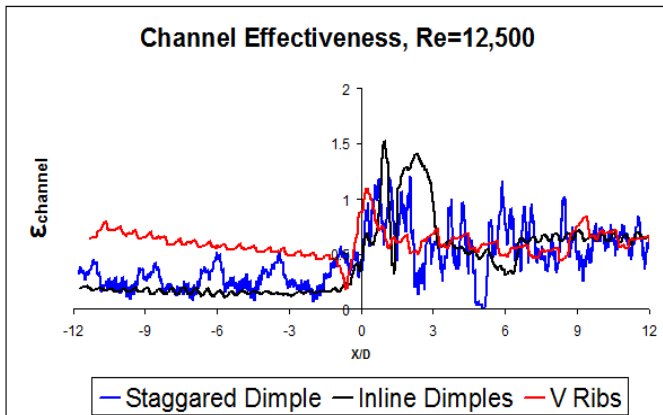


Figure 8: Channel Effectiveness distribution along the length of the channel for the three geometric configurations, at $Re=12,500$

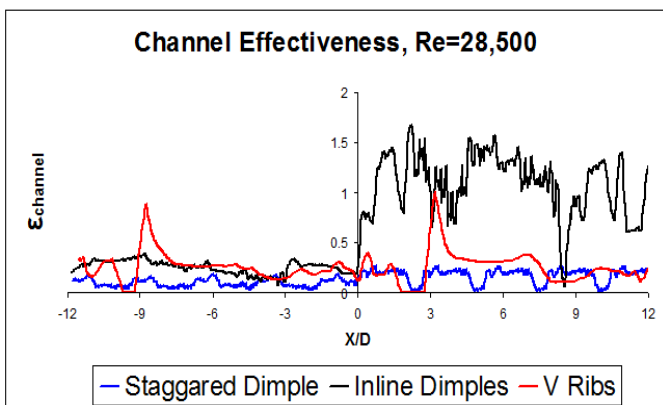


Figure 9: Channel Effectiveness distribution along the length of the channel for the three geometric configurations, at $Re=28,500$

Higher heat transfer and lower friction coefficient is desired in any channel and this translates to higher channel effectiveness. Figures 8 and 9 show the distribution of channel effectiveness for the three channels along the length. The effectiveness is very small in the upstream section of the bend compared to the downstream. This is because the heat transfer is much higher in the downstream section, owing to a higher turbulence caused by the flow bend. Unlike the heat transfer, the friction reduces in the downstream section due to a flow separation and the resulting recirculation of the flow. Comparing the different turbulators, the staggered dimpled channel performs better than the inline dimpled channel and

both the dimpled channel perform better than the ribbed channel. Also, at higher Reynolds number, channel effectiveness improves, for the inline dimple case but not ribbed and staggered dimples.

Comparing the dimpled channels alone, the poor performance of the staggered channel can be attributed to the increase in friction without much gain in the heat transfer.

CONCLUSIONS

From this study, the following conclusions emerged:

- (1) The dimpled channel performs better cooling effectiveness when compared with the V-ribbed channel. However, if the friction is reduced in ribbed channels, the ribbed channel is better suited.
- (2) Comparing the channel effectiveness, both the ribbed channel and the staggered dimpled channel perform equally and the inline channel performs better than the other two, at higher Reynolds number.
- (3) For $Re_D = 12,500$, the V-ribs perform marginally better than the dimpled channel in the upstream side and all three channels perform similarly in the downstream side.

To better understand the performance, more studies need to be performed through both experimental and computational studies for various possible geometries. Some of the geometric configurations that need to be studied are the ribs at different angles, depressed ribs, convex dimples and circular ribs.

ACKNOWLEDGMENTS

This work was supported through UWM Development Fund.

REFERENCES

1. Bunker R., 2008 “Chapter 7: Innovative Gas Turbine Cooling” In Amano R., Suden B. (Ed), in Thermal Engineering in Power Systems Billerica, MA, WIT Press

2. Iacovides, H., Launder, B. E., Li, H.Y., 1996 "The computation of flow development through stationary and rotating U-ducts of strong curvature" International Journal of Heat and Fluid Flow, Volume 17, Issue 1, pp. 22-33
3. Ekkad, S. V., Huang, Y and Han, JC, 1998 "Detailed Heat Transfer Distribution in Two-Pass Square Channels With Rib Turbulators and Bleed Holes", Intl. J of Heat Transfer **41**, pp. 3781-3791
4. Kim, K. M., Park S., Jeon H, Lee D., and Cho H. 2008 "Heat/Mass Transfer Characteristics In Angled Ribbed Channels With Various Bleed Ratios And Rotation Numbers." J. Turbomach. 130, 031021.
5. Han, J.C. and Ekkad, S. V., 1995 "Detailed Heat Transfer Distributions in Two-Pass Square Channels with Rib Turbulators", Int. J of Mass Transfer, Vol **40**, No 11, pp. 2525-2537.
6. Zhou, F. and Acharya, S. 2009 "Experimental and Computational Study of Heat/Mass Transfer and Flow Structure for Four Dimple Shapes in a Square Internal Passage", Proc. Of ASME Turbo Expo Orlando, Fl, ASME Paper GT2009-60240
7. Moon, H.K, O'Connell, T., Glezer, B., 2000 "Channel Height Effect on Heat Transfer and Friction in a Dimpled Passage" Journal of Engineering for Gas Turbines and Power, **122**, pp. 307-313
8. Amano, R.S., Guntur, K.S. and Lucci, J.M., 2009 "Computational Study of Heat Transfer Characteristics in a Ribbed Cooling Channel" 7th Annual International Energy Conversion Engineering Conference, Denver CO, ASME Paper DETC2009-87423
9. Lucci, J.M., Guntur K.S., Amano R. 2007 "Turbulent Flow and Heat Transfer In Variable Geometry U-Bend Blade Cooling Passage", ASME Turbo Expo, Montreal, ASME Paper GT2007-27120
10. Guntur K.S., Lucci, J.M., and Amano R., 2007, A Computational Study of turbulent flow and heat transfer through $Rc/D = 3.357$ U Bend cooling passage of a Gas Turbine Blade, ASME IDETC/CIE, Las Vegas, NV, ASME Paper DETC 2007-35140
11. Lucci, J.M., Amano R. and Guntur K., 2007, A Computational Study on Turbulent flow and heat transfer in a strongly curved $Rc/D = 0.65$ turbine blade cooling passage Jose Martinez ASME IDETC/CIE, Las Vegas, NV, ASME Paper DETC 2007-35143
12. Guntur, K.S., Amano, R.S., Kumar, S. and Lucci, J.M., 2010 "Comparison Of $k-\epsilon$ And $k-\omega$ Models With Experiment For Heat Transfer In A Cooling Channel With Dimples", Proceedings of IMECE ,Vancouver, British Columbia, ASME Paper IMECE2010-37535
13. Amano R S, 1982 "Numerical Study of Liquid Cooling Gas Turbine Blade" IGTI Proceedings, London, 82-GT-116
14. Jayatilke, C. L, 1969 " The Influence of Prandtl Number and Surface Roughness on The Resistance of Laminar Sublayer to Momentum Heat Transfer" Progress In Heat And Mass Transfer, **1**, pp. 193-329